Am J Cancer Res 2020;10(3):965-974
www.ajcr.us /ISSN:2156-6976/ajcr0107226

Original Article

MicroRNA-590-3p inhibits invasion and metastasis in triple-negative breast cancer by targeting Slug

Meisi Yan[3,6*], Leiguang Ye[2*], Xinxin Feng[3], Runze Shi[1], Zhen Sun[4], Zhigao Li[1#], Tong Liu[1,5#]

Departments of [1]Breast Surgery, [2]Oncology, Harbin Medical University Cancer Hospital, Harbin 150000, China; [3]Department of Pathology, Harbin Medical University, Harbin 150081, China; [4]Department of Molecular and Cellular Biology, Baylor College of Medical, TX 77030, United States; Departments of [5]Pathology, [6]Molecular and Cellular Oncology, The University of Texas MD Anderson Cancer Center, TX 77030, United States. [#]Equal contributors. [*]Co-first authors.

Received December 17, 2019; Accepted February 20, 2020; Epub March 1, 2020; Published March 15, 2020

Abstract: miR-590-3p acts as a tumor suppressor in glioblastoma multiform, medulloblastoma, hepatocellular carcinoma, and nephroblastoma. Here, we studied the role of miR-590-3p in triple-negative breast cancer (TNBC). The miR-590-3p levels in TNBC specimens were significantly lower than those in non-TNBC specimens. Overexpression of miR-590-3p significantly inhibited migration and invasion of TNBC cells and lung metastasis *in vivo*. Interestingly, miR-590-3p decreased the Slug mRNA and protein levels in TNBC cells, and luciferase reporter assay showed that miR-590-3p directly targeted 3'-UTR of Slug in TNBC cells. Importantly, overexpression of Slug reversed the inhibitory effect of miR-590-3p on migration and invasion of TNBC cells. Taken together, miR-590-3p inhibits TNBC migration and invasion by directly targeting Slug, suggesting a potential therapeutic effect of miR-590-3p for TNBC.

Keywords: Triple-negative breast cancer, cancer metastasis, miR-590-3p, Slug

Introduction

Breast cancer is a commonly diagnosed malignancy in women and has high mortality rates [1]. Although targeted treatment has greatly improved the survival rate of patients with breast cancer, effective targeted therapies are limited for triple-negative breast cancer (TNBC), which is negative for human epidermal growth factor receptor 2, progesterone receptor, and estrogen receptor. TNBC is a highly aggressive type of breast cancer that frequently metastasizes to multiple sites [2]. The high metastatic rate of TNBC is associated with poor clinical outcomes of patients with TNBC [3].

Tumor metastasis is a complex, multiscale process that is involved in the invasion of primary tumor cells to the adjacent tissues or distant tissues via the blood circulation. The growth of tumor cells at the distant sites results in metastasis clinically identifiable [4]. A crucial step that contributes to the invasiveness of tumor cells is the epithelial-mesenchymal transition (EMT), which inhibits cell-to-cell adhesion and enhances their ability to migrate, invade, and survive in the peripheral circulation [5-7]. Slug (SNAIL2) is one of the key regulators of EMT and inhibits transcription of the epithelial marker E-cadherin [8]. A better understanding of the molecular mechanisms underlying TNBC progression and metastasis is critical for developing effective treatment strategies for this disease.

MicroRNAs (miRNAs) are aberrantly expressed in breast cancer, gastric cancer, leukemia, and other diseases, where miRNAs directly impact the expression of their target genes [9-11]. These small non-coding RNAs are intricately associated with cancer initiation and development, several of which having been identified as tumor suppressors or oncogenes [12]. For instance, miR-10b and miR-335 are among the earliest miRNAs reported to function as an inhibitor and a promoter of metastasis, respectively; miR-200b, miR-183, miR-494, and let-7a have also been implicated in the invasion-metastasis cascade [13-16]. Recently, it has also been reported that miR-590-3p is up-regulated

in nephroblastoma, lung adenocarcinoma, lymphoblastic leukemia, and glioblastoma multiforme [17-20]. Furthermore, miR-590-3p was found to inhibit colorectal cancer tumorigenesis by targeting YAP1 [21] and target the transcriptional enhancer activator domain 1 in liver cancer, indicating its potential as a diagnostic/prognostic marker for hepatocellular carcinoma [22]. However, the role of miR-590-3p in TNBC has not been fully understood.

In this study, miR-590-3p was detected to be down-regulated in TNBC tumors. Exogenous expression of miR-590-3p in TNBC cells significantly inhibited the invasiveness and motility of TNBC cells *in vitro* and metastasis *in vivo*. miR-590-3p inhibited TNBC migration and invasion by targeting Slug, a key regulator of EMT.

Materials and methods

Cell lines and cell culture

The immortalized breast epithelial cell line MCF-10A and the human breast cancer cell lines BT-549 and MDA-MB-231 were purchased from the Chinese Academy of Sciences (Shanghai, China). SKBR3 and MCF-7 cell lines were obtained from American Type Culture Collection (Manassas, VA, USA). Leibovitz L-15 medium (Gibco Laboratories, MD, USA) was used to culture MDA-MB-231 cells, RPMI 1640 (Hyclone, USA) for BT-549 cells, and Dulbecco's modified Eagle's medium (Hyclone Laboratories Inc., USA) for the immortalized human embryonic kidney cell line HEK293T. All culture media were supplemented with 10% fetal bovine serum FBS and 1% antibiotics (Gibco Laboratories). All cell lines were cultured in 5% CO_2 at 37°C in a cell culture incubator except that MDA-MB-231 cells were grown in 100% air.

Patients and breast tissue samples

Forty-two TNBC and 18 non-TNBC tumor tissue specimens were harvested from patients during surgical resection at the Harbin Medical University Cancer Hospital in Harbin, China. Written consent was obtained from all patients, and the tissue samples were confirmed by histological examination. The patients were followed up for at least five years, starting from 2009. The Scarff-Bloom-Richardson system (Elston-Ellis modification) was used to grade the tumors histologically. The American Joint Committee on Cancer criteria was used to determine the clinical and tumor stages and clinic-pathological classification. All experiments and protocols adhered to the ethical standards outlined in the Declaration of Helsinki.

Luciferase reporter assay

The binding of miR-590-3p to Slug mRNA in TNBC cells was determined using a luciferase reporter assay. The putative miR-590-3p complementary site in the 3'-UTR of Slug mRNA or its mutant sequence was cloned into the psiCHECK-2 luciferase reporter vector (Promega, Madison, WI, USA). TNBC cells were co-transfected with 60 pmol of miR-590-3p mimic or miR-590-3p-NC and 4 μg of psiCHECK-2-Slug-3'UTR-WT or psiCHECK-2-Slug-3'UTR-MUT. The cells were collected at 48 h after transfection and analyzed using the Dual-Luciferase Reporter Assay System (Promega). The firefly and Renilla luciferase signals were detected using the GloMax fluorescence reader (Promega). The Renilla luciferase signal was normalized to the firefly luciferase signal.

Plasmid transfection

In pcDNA3.1-HA, annealed oligonucleotides encoding the HA tag were ligated into the HindIII and BamHI sites of pcDNA3.1 (Invitrogen). The ORF of human Slug was generated from MDA-MB-231 cells, and the resultant PCR product was connected with pcDNA3.1 tagged HA (Slug-HA). miR-590-3p mimic (5'-UAAUUUUAUGUAUAAGCUAGU-3') and miR-590-3p-negative control (miR-590-3p-NC) (3'-AUUAAAAUACAUAUUCGAUCA-5') were synthesized by RiboBio (Guangzhou, China). miR-590-3p-NC and scrambled RNA (MISSION siRNA Universal Negative Control; Sigma-Aldrich, St. Louis, USA) were used as the negative controls. The cells were transfected with 10 μg of miR-590-3p mimic, miR-590-3p-NC, or scrambled RNA with or without 4 μg of Slug using the miRNA Transfection X-treme GENE Reagent (Roche, USA) for 6 h at 37°C. The medium was then replaced with fresh medium containing 10% FBS, and the cells were cultured for 48 h. At 48 h post-transfection, Real-time PCR (RT-PCR) and Western blotting were performed.

RNA extraction and quantitative real-time PCR

The expression levels of miR-590-3p in TNBC cell lines and tumor tissues of patients with

TNBC were determined using quantitative real-time PCR (qRT-PCR). The cDNA templates for qRT-PCR were synthesized from RNA samples. All primers sequences were as follows: miR-590-3p forward 5'-GCAGTGGAATGTAAGGAAGTGTGT-3', reverse 5'-GCGAGCACAGAATTAATACGACTC-3'; For miRNA detection, miRNA was reversely transcribed using the TaqMan MicroRNA Reverse Transcription kit, and real-time quantitative PCR was performed using TaqMan miR-590-3p and U6 RNA (used as a normalizer) assays (Life Technologies) following the manufacturer's instructions. Slug (R): 5'-GTGTTTGCAAGATCTGCGGC-3'; Slug (F): 5'-GAGCCCTCAGATTTGACCTGT-3'. Gene expression was determined using 0.2 μg of the template and SYBR Green I (Toyobo, Osaka, Japan) with the ABI 7500 fast system (Applied Biosystems, CA, USA). qRT-PCR was performed on a MyiQ.2 Two-Color Real-Time PCR Detection System (Bio-Rad Laboratories, CA, USA) using the following amplification conditions: 5 min 95°C followed by 40 cycles of 10 seconds 95°C, 20 seconds 60°C, and 20 seconds 72°C. The relative expression levels of the genes were normalized using the $2^{-\Delta\Delta C}_{T}$ methods.

Cell proliferation assay

Cell proliferation was assessed using the CCK-8 assay kit (Dojindo Molecular Technologies, Shanghai, China) according to the manufacturer's protocol. Briefly, 2×10^4 cells/well in 100 mL complete medium were seeded into 96-well plates At 0, 24, 48, and 72 h after incubation at 37°C with 5% CO_2, 10 μL CCK-8 solution was added to each well. The plates were incubated for another 2 h at 37°C in 5% CO_2, and the absorbance at 450 nm was measured using a Microplate Reader (Bio-Rad Laboratories, CA, USA).

Cell invasion assay

Cell invasion was assessed using the BioCoat Matrigel Invasion Chamber (BD Biosciences, MA, USA) and 8 μm-pore size Transwell chambers (Corning Inc., NY, USA). The cells were seeded in the upper chambers in serum-free media at the density of 1×10^5 cells/well (invasion assay), and the lower chambers were filled with complete media as attractants. After incubation at 37°C with 5% CO_2 for 24 h, the non-invaded cells were removed from the upper surface of the Transwell membrane with a cotton swab, and the invaded cells on the lower surface of the membrane were fixed with 600 μL of 70% ethanol at room temperature for 10 min and stained with 600 μL of 0.1% crystal violet (Invitrogen, CA, USA) at room temperature for 10 min. Then images of the stained cells were taken (magnification, ×200), and the stained cells were counted under an Olympus IX73 routine light microscope (Olympus Corporation, Japan).

Wound healing assay

The cells were seeded into 24-well plates and cultured until they were 100% confluent. The monolayer was gently scratched with a sterile tip to create a "wound field". The wound area was photographed at 0 h and 24 h after scratching, and the distance traveled by the cells across the wound was evaluated microscopically. The migration rate was defined as the fraction of cell coverage across the wound. The cells migrated from the wound edge were counted.

Western blotting

Cells were lysed in RIPA lysis buffer containing protease inhibitor cocktail. Total protein concentration was determined using Pierce BCA Protein assay kit (Thermo Fisher Scientific, MA, USA). The cell lysates were electrophoresed in 10% sodium dodecyl sulfate-polyacrylamide gels and transferred onto polyvinylidene difluoride membranes (Millipore, MA, USA). The membranes were subsequently blocked with 5% non-fat milk-TBST solution for 1 h and incubated overnight at 4°C with anti-Slug (1:1000, #9585, Cell Signaling Technology, MA, USA), anti-vimentin (1:1000, #ab92547, Abcam, Cambridge, UK), anti-E-Cadherine (1:1000, #ab-1416, Abcam, Cambridge, UK), anti-β-actin (1:3000, 20536-1-AP, Proteintech, IL, USA) primary antibodies. After washes with TBST buffer, the membranes were incubated with a horseradish peroxidase-conjugated secondary antibody for 1 h at room temperature. The blots were developed using the ECL kit (Millipore, WI, USA). The experiment was repeated three times.

TNBC xenograft metastatic mouse model

All animals were maintained and handled in accordance with the guidelines of the Animal

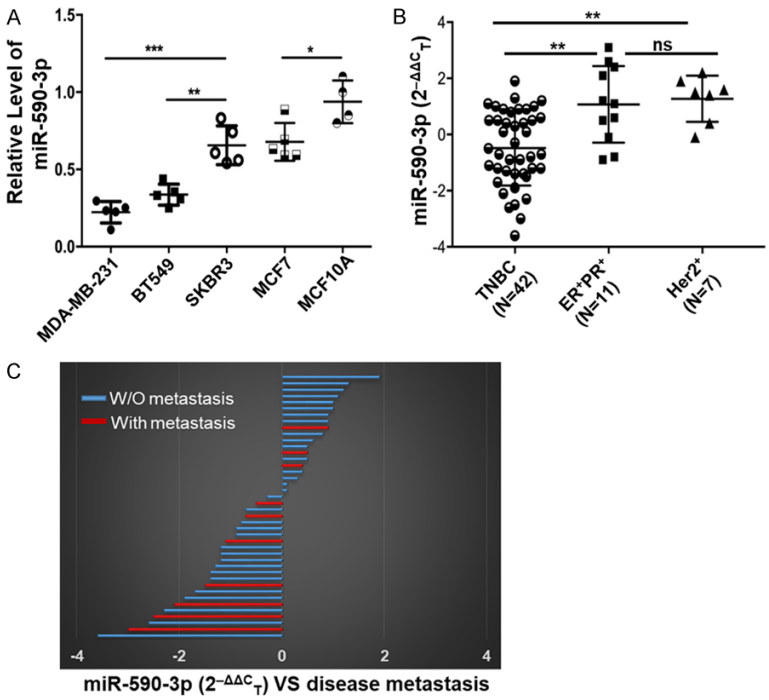

Figure 1. Expression levels of miR-590-3p are down-regulated in breast cancer specimens and cell lines. A. Levels of miR-590-3p in breast cancer cell lines and human mammary epithelial cells, as determined using qRT-PCR. B. Levels of miR-590-3p in TNBC (n = 42) and non-TNBC (n = 18) tumor tissues, as determined using qRT-PCR. C. Frequency of distant organ metastasis (lung, bone and liver) 5 years post-surgery in TNBC patients with the miR-590-3p^{high} or miR-590-3p^{low} tumors. Data are presented as mean ± SD from three independent experiments. The differences in expression levels of miR-590-3p between different cell lines or between different tumor tissues were analyzed using one-way ANOVA and followed by the SNK test. Median values are represented by the horizontal line in the middle. *, $P < 0.05$ was considered statistically significant, denoted by **, $P < 0.01$; ***, $P < 0.001$; and ns, no significance.

Care and Use Committee of Harbin Medical University. Luciferase-labeled MDA-MD-231 control cells and miR-590-3p-overexpressing MDA-MB-231 cells (2×10^6) were injected into the tail veins of 6-week-old female nude mice (n = 5 per group). Pulmonary metastasis was monitored weekly by the live animal Lumina II system (Xenogeny IVIS system).

Bioinformatics

Potential targets of hsa-miR-590-3p in the 3'-UTR of EMT-inducing transcription factors were identified by bioinformatics analysis, based on the target prediction tools Target Scan (version 6.0, November 2011, Whitehead Institute for Biomedical Research) and the miRanda program (August 2010 Release, Memorial Sloan-Kettering Cancer Center).

Statistical analysis

All data are presented as mean ± SD from three independent experiments. The differences in expression levels of miR-590-3p between different cell lines and between different breast tumor tissues were analyzed using one-way ANOVA and followed by Student-Newman-Keuls (SNK) test. The differences in migration, invasion, and metastasis between the miR-590-3p-NC cells and the miR-590-3p-mimics cells were analyzed using two-tailed Student's *t*-test. The correlations between the mRNA levels of Slug and the expression levels of miR-590-3p in TNBC tumors or between the expression levels of miR-590-3p and TNBC metastasis rates were analyzed using Pearson test correlation coefficients. Statistical analyses were performed using the GraphPad Prism 7.0 (Prism Software Inc., San Diego, USA). A value of $P \leq 0.05$ was considered statistically significant. NS, not significant; no statistical methods were used to predetermine sample size.

Results

miR-590-3p is down-regulated in TNBC tumors and cell lines

To determine the role of miR-590-3p in breast cancer, we first assessed the miR-590-3p in breast cancer tissues and cell lines by qRT-PCR. miR-590-3p levels were around 1.8-fold, 2-fold, and 2.5-fold lower in BT-549 TNBC cells compared to SKBR3 (non-TNBC), MCF-7 (non-TNBC), and MCF-10A (immortalized normal breast epithelial cell line), respectively (**Figure 1A**). In MDA-MB-231 TNBC cells, miR-590-3p levels were around 3-fold, 3.2-fold, and 4-fold lower compared to SKBR3 (non-TNBC), MCF-7 (non-TNBC), and MCF-10A (immortalized normal bre-

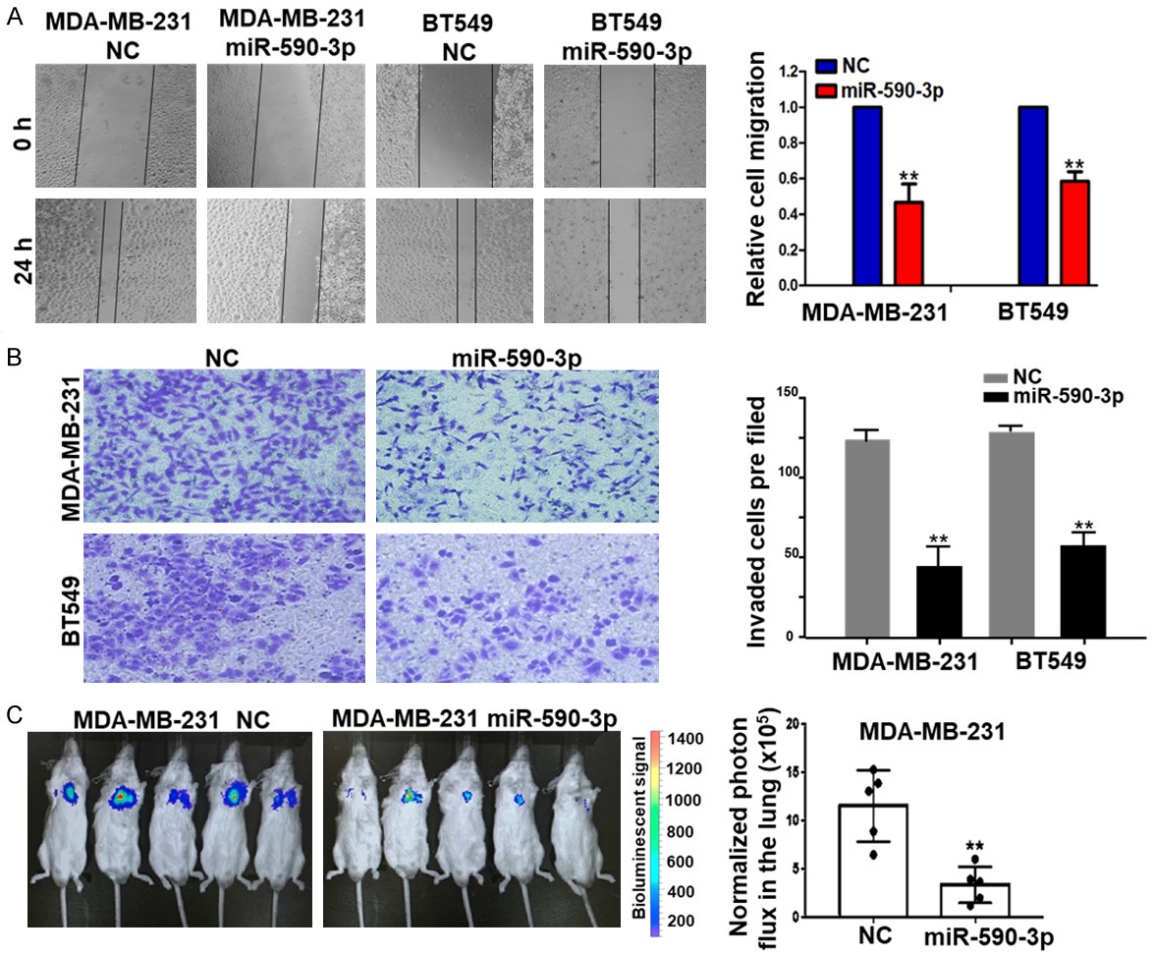

Figure 2. Overexpression of miR-590-3p inhibits migration and invasion of TNBC cells *in vitro* and metastasis *in vivo*. A. Representative images of wound healing assay (left panel) show the migration of MDA-MB-231 and BT-549 cells transfected with miR-590-3p-NC or miR-590-3p mimics, at the beginning (t = 0 h) and the end (t = 24 h) of the recording. The graph (right panel) shows the numbers of the migrated cells transfected with miR-590-3p mimics or miR-590-3p-NC. **, $P < 0.01$. B. Representative images of transwell assay (left panel) show the invasion of MDA-MB-231 and BT549 cells transfected with miR-590-3p-mimics or miR-590-3p-NC. The graph (right panel) shows the numbers of the invaded cells transfected with miR-590-3p mimics or miR-590-3p-NC. **, $P < 0.01$. C. Representative IVIS images (left panel) show lung metastases in mice that were injected with luciferase-labeled MDA-MB-231 cells transfected with miR-590-3p mimics or the miR-590-3p-NC control. The graph (right panel) shows quantitation of lung metastases on day 40 after implantation of tumor cells, as assessed by bioluminescence measurements (n = 5). The color scale bar depicts the photon flux (photons per second) emitted from these mice. Data are presented as mean ± SD from three independent experiments. The differences in migration, invasion, and metastasis between the miR-590-3p-NC and the miR-590-3p-mimic cells were analyzed using two-tailed Student's *t*-test. **, $P < 0.01$ was considered statistically significant.

ast epithelial cell line), respectively (**Figure 1A**). Consistently, miR-590-3p levels in TNBC patient tumor tissues (n = 42) were around 3-fold lower than those in non-TNBC tumor tissues (n = 18) (**Figure 1B**, $P < 0.01$). Furthermore, the incidence of distant metastasis in the lung, bone, and liver 5 years post-surgery was significantly higher in TNBC patients with tumors that have low levels of miR-590-3p than in patients with tumors that have high levels of miR-590-3p (**Figure 1C**), indicating that miR-590-3p may play an important role in TNBC.

miR-590-3p inhibits migration and invasion of TNBC cells in vitro and metastasis in vivo

To determine the role of miR-590-3p in TNBC cell migration and invasion, we transfected BT-549 and MDA-MB-231 cells with miR-590-3p mimics or miR-590-3p-NC control. The effect

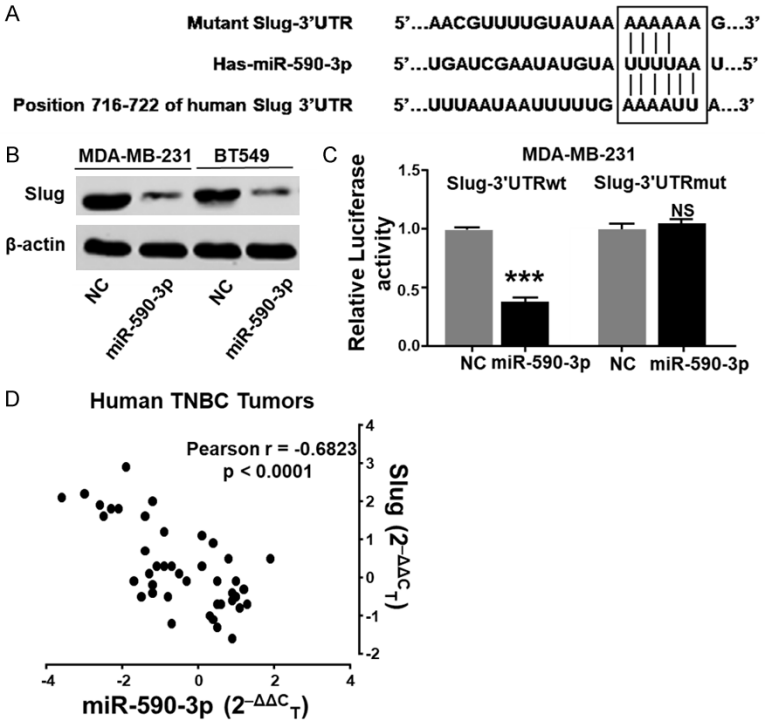

Figure 3. miR-590-3p directly targets Slug, and its expression level is correlated with a high metastasis rate in TNBC patients. A. RNA sequence alignment shows that the 3'-UTR of Slug mRNA contains a complementary site for the seed region of miR-590-3p. Slug-mut, a mutant with substitutions in the complementary region, was used as a negative control. B. Enforced expression of miR-590-3p suppressed the expression of Slug protein in TNBC cell lines, as determined by Western blotting. C. The luciferase activity was determined using dual luciferase reporter assay after transfection of the luciferase reporter vector (psiCHECK-2-Slug-3'UTR-WT or psiCHECK-2-Slug-3'UTR-MUT) into miR-590-3p-mimic or miR-590-3p-NC-transfected MDA-MB-231 cells. The data represent the means ± SD of three independent experiments. The luciferase activity was measured. Data are presented as mean ± SD from three independent experiments; ***, $P < 0.001$ compared with the negative control; and ns, no significance. D. The mRNA levels of Slug were reversely correlated with the expression levels of miR-590-3p in TNBC tissue specimens (n = 42), as determined by qRT-RCR. The correlation between the mRNA levels of Slug and the expression levels of miR-590-3p in TNBC tumors were analyzed using Pearson test. $P < 0.001$ was considered statistically significant.

of miR-590-3p overexpression on cell migration was determined using the wound healing assay, Compared with the miR-590-3p-NC control, miR-590-3p overexpression significantly reduced migration (**Figure 2A**) of both BT549 cells (2-fold reduction, $P < 0.01$) and MDA-MB-231 cells (2.3-fold reduction, $P < 0.01$). The effect of miR-590-3p overexpression on cell invasion was determined using the transwell assay. Compared with the miR-590-3p-NC control, miR-590-3p overexpression significantly reduced invasion (**Figure 2B**) of both BT549 cells (2.2-fold reduction, $P < 0.01$) and MDA-MB-231 cells (2.5-fold reduction, $P < 0.01$). Additional cell proliferation studies showed that miR-590-3p overexpression did not inhibit cell growth for up to 24 h post transfection in both BT-549 and MDA-MB-231 cell lines (Supplementary Figure 1). This result confirms that the inhibitory effects of miR-590-3p overexpression on cell migration and invasion are not a result of growth inhibition.

We further tested the role of miR-590-3p in TNBC metastasis using a TNBC mouse model. Luciferase-labeled MDA-MB-231 cells overexpressing either miR-590-3p or miR-590-3p-NC were injected into female nude mice via the tail vein. On day 40 after tumor cell injection, the luciferase signals detected in the lungs were 3.91-fold lower in mice bearing miR-590-3p-overexpressing tumors than in mice bearing miR-590-3p-NC-overexpressing tumors (**Figure 2C**, $P < 0.01$). This result suggests that miR-590-3p overexpression significantly reduced lung metastases.

miR-590-3p directly targets Slug

To identify the targets of miR-590-3p, we performed bioinformatics analysis using Targetscan and miRanda programs and identified Slug as the top candidate. To validate that Slug is indeed a direct target of miR-590-3p and that miR-590-3p regulates Slug expression, we constructed a luciferase reporter containing the complementary seed sequence of miR-590-3p in the 3'-UTR region of Slug mRNA (**Figure 3A**) and a control reporter of Slug containing the mutated sequence of the same fragment. We then assessed the effects of miR-590-3p overexpression on the expression of Slug at protein levels in both MDA-MB231 and BT549 cells by Western blotting. Slug protein levels were dramatically down-regulated in both MDA-MB231 and BT549 cells

stably overexpressing miR-590-3p (**Figure 3B**). Compared to that in the MDA-MB-231 control cells, luciferase activity was reduced by 60% in MDA-MB-231 cells co-transfected with the miR-590-3p and the luciferase reporter ($P < 0.001$). In contrast, luciferase activities were comparable between the MDA-MB-231 control cells and the cells co-transfected with the control reporter (**Figure 3C**), indicating that miR-590-3p failed to inhibit luciferase activity of the control reporter containing the mutated sequence of the 3'-UTR region of Slug mRNA. These results demonstrate that Slug is the direct target of miR-590-3p. Furthermore, a strong inverse correlation was found between the expression levels of miR-590-3p and the mRNA levels of Slug in the TNBC tumors (**Figure 3D**; Pearson r = -0.6823, $P < 0.0001$).

Slug reverses the inhibitory effect of miR-590-3p on EMT in TNBC

Given that miR-590-3p suppressed migration, invasion, and metastasis of TNBC cells and that Slug was a target of miR-590-3p, we then examined whether miR-590-3p regulates TNBC metastasis through suppressing Slug and whether Slug overexpression reverses the effect of miR-590-3p on EMT. To test our hypothesis, we co-transfected TNBC cells with miR-590-3p-NC or miR-590-3p mimic along with the vector carrying Slug-coding sequence and then assessed the effects on cell migration and invasion (**Figure 4A** and **4B**). Compared to the control cells, miR-590-3p-overexpressing MDA-MB-231 and BT-549 cells exhibited an up-regulated expression of the epithelial marker E-Cadherin and down-regulated expression of the mesenchymal markers Slug and Vimentin, as determined by Western blotting (**Figure 4B**). Overexpression of Slug reversed the effects of miR-590-3p on the expression of E-Cadherin and Vimentin (**Figure 4B**). More importantly, miR-590-3p overexpression suppressed migration (**Figure 4C**) and invasion (**Figure 4D**) of both MDA-MB-231 and BT-549 cells, whereas Slug overexpression reversed the inhibitory effects of miR-590-3p on migration and invasion (**Figure 4C** and **4D**). Interestingly, additional studies revealed that not only could Slug reverse the inhibitory effect of miR-590-3p on cell migration and invasion, it also abolished the inhibition of miR-590-3p on cell proliferation at 48 h and 72 h in both TNBC cell lines tested (Supplementary Figure 2). Together, these results indicate that miR-590-3p inhibits the invasiveness of TNBC cells by suppressing the EMT phenotype.

Discussion

Despite considerable advancements in treating localized malignancies, effective targeted therapies against metastatic TNBC, the major contributor to breast cancer-related mortality, are limited [23]. It is essential to understand the mechanisms underlying TNBC metastasis to identify novel therapeutic targets for the development of targeted therapies for TNBC. Critical for a myriad of physiological developments, EMT is characteristic of the initiation of metastasis in cancer progression. Slug, one of the key regulators of EMT, suppresses E-cadherin expression and subsequently reduces intercellular adhesion and increases cell motility [24]. Furthermore, Slug is degraded upon binding to p21 and p53, which are well-known tumor suppressors that inhibit cancer cell invasion [25].

There has been an increasing focus on miRNAs as cancer therapeutics. miRNAs have an advantage over other anti-cancer therapies since they can be easily administered via parenteral or local injection routes, with satisfactory tissue penetration. Over 500 patents related to miRNAs are filed every year [26]. For instance, miRNA-34 is currently in a phase I trial for testing its therapeutic application in liver cancer [26]. The low levels of miR-34a in an orthotopic model of hepatocellular carcinoma were restored by administering exogenous miR-34a using NOV340 liposome [27], which inhibited cancer initiation and proliferation, and promoted apoptosis.

In this study, we found that the levels of miR-590-3p were significantly lower in the TNBC tumor tissues than those in non-TNBC tumor tissues. We also found that the low levels of miR-590-3p correlated with a high metastasis rate and high Slug expression in TNBC. Furthermore, overexpression of miR-590-3p in the TNBC cells markedly suppressed migration and invasiveness of tumor cells *in vitro* and significantly inhibited lung metastases *in vivo* in the mouse model. Our mechanism study indicates that miR-590-3p inhibits TNBC metastasis by suppressing Slug-mediated EMT, a key step of tumor metastasis. Taken together, our findings warrant further investigations of miR-590-3p as a potential therapeutic agent for TNBC.

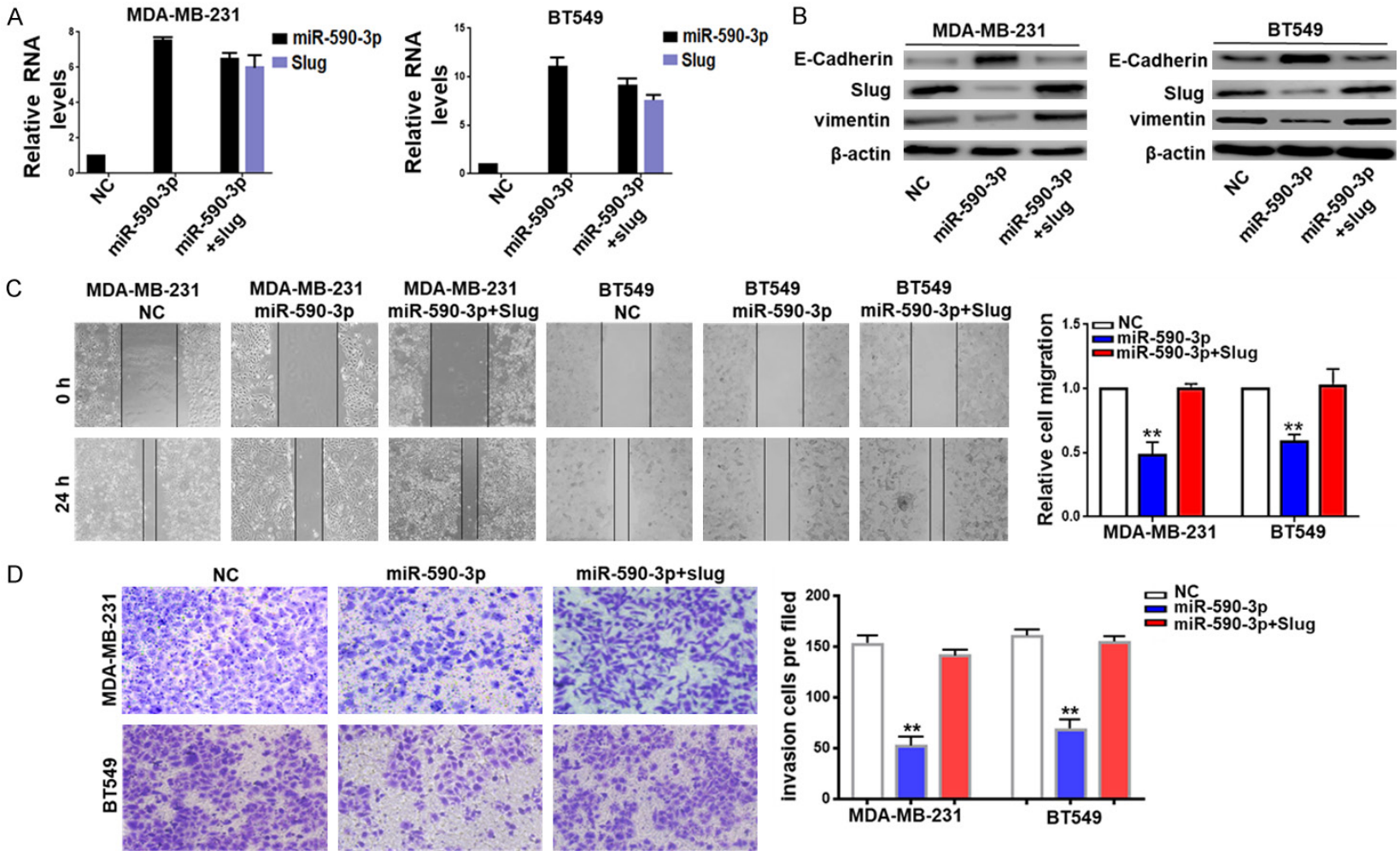

Figure 4. miR-590-3p inhibits the EMT phenotype by suppressing Slug expression in TNBC cells. (A) Expression levels of miR-590-3p and Slug mRNA in MDA-MB-231 and BT-549 cells were determined using qRT-PCR after transfection with miR-590-3p-NC or miR-590-3p mimic along with or without the Slug. (B) Western blots show the protein expression levels of Slug, E-cadherin, and Vimentin in MDA-MB-231 and BT-549 cells, which were transfected with miR-590-3p-NC or miR-590-3p mimic along with or without the Slug. β-actin was used as a loading control. (C) Representative images (left panel) show the migration of BT-549 and MDA-MB-231 cells after transfection with miR-590-3p-NC or miR-590-3p mimic along with or without the Slug at 0 h and 24 h of recording of migration. The graph (right panel) shows that the inhibitory effect of miR-590-3p on cell migration was largely reversed by Slug overexpression. **, $P < 0.01$. (D) Representative images show the invasion of MDA-MB-231 and BT549 cells after transfection with miR-590-3p-NC or miR-590-3p mimic along with or without the Slug. The graph (right-lower panel) shows that the inhibitory effect of miR-590-3p on cell invasion was largely reversed by Slug overexpression. **, $P < 0.01$. In (C and D), differences in migration and invasion among cells transfected with miR-590-3p-NC or miR-590-3p mimic along with or without the Slug. were analyzed using two-tailed Student's *t*-test. **, $P < 0.01$ was considered statistically significant.

Acknowledgements

This study was supported by the National Natural Science Foundation of China Youth Project (81802647), the National Natural Science Foundation of China (81872157), the Natural Science Foundation of Heilongjiang Province of China (QC2017111) and the Health and Family Planning Commission of Heilongjiang province (Grant No. 2017-159).

Disclosure of conflict of interest

None.

Address correspondence to: Drs. Tong Liu and Zhigao Li, Department of Breast Surgery, Harbin Medical University Cancer Hospital, Harbin 150000, China. Tel: +86-0451-86298091; E-mail: liutong@hrbmu.edu.cn (TL); drzhigaoli@hrbmu.edu.cn (ZGL)

References

[1] Burnett RM, Craven KE, Krishnamurthy P, Goswami CP, Badve S, Crooks P, Mathews WP, Bhat-Nakshatri P and Nakshatri H. Organ-specific adaptive signaling pathway activation in metastatic breast cancer cells. Oncotarget 2015; 6: 12682-12696.

[2] Fidler IJ. The pathogenesis of cancer metastasis: the 'seed and soil' hypothesis revisited. Nat Rev Cancer 2003; 3: 453-458.

[3] Bianchini G, Balko JM, Mayer IA, Sanders ME and Gianni L. Triple-negative breast cancer: challenges and opportunities of a heterogeneous disease. Nat Rev Clin Oncol 2016; 13: 674-690.

[4] Valastyan S and Weinberg RA. Tumor metastasis: molecular insights and evolving paradigms. Cell 2011; 147: 275-292.

[5] Yeh YW, Cheng CC, Yang ST, Tseng CF, Chang TY, Tsai SY, Fu E, Chiang CP, Liao LC, Tsai PW, Yu YL and Su JL. Targeting the VEGF-C/VEGFR3 axis suppresses Slug-mediated cancer metastasis and stemness via inhibition of KRAS/YAP1 signaling. Oncotarget 2017; 8: 5603-5618.

[6] Hanahan D and Weinberg RA. Hallmarks of cancer: the next generation. Cell 2011; 144: 646-674.

[7] Fedele M, Cerchia L and Chiappetta G. The epithelial-to-mesenchymal transition in breast cancer: focus on basal-like carcinomas. Cancers (Basel) 2017; 9.

[8] Polyak K and Weinberg RA. Transitions between epithelial and mesenchymal states: acquisition of malignant and stem cell traits. Nat Rev Cancer 2009; 9: 265-273.

[9] Markopoulos GS, Roupakia E, Tokamani M, Chavdoula E, Hatziapostolou M, Polytarchou C, Marcu KB, Papavassiliou AG, Sandaltzopoulos R and Kolettas E. A step-by-step microRNA guide to cancer development and metastasis. Cell Oncol (Dordr) 2017; 40: 303-339.

[10] Farazi TA, Hoell JI, Morozov P and Tuschl T. MicroRNAs in human cancer. Adv Exp Med Biol 2013; 774: 1-20.

[11] Sato-Kuwabara Y, Melo SA, Soares FA and Calin GA. The fusion of two worlds: non-coding RNAs and extracellular vesicles--diagnostic and therapeutic implications (Review). Int J Oncol 2015; 46: 17-27.

[12] Asghari F, Haghnavaz N, Baradaran B, Hemmatzadeh M and Kazemi T. Tumor suppressor microRNAs: targeted molecules and signaling pathways in breast cancer. Biomed Pharmacother 2016; 81: 305-317.

[13] Zheng Q, Cui X, Zhang D, Yang Y, Yan X, Liu M, Niang B, Aziz F, Liu S, Yan Q and Liu J. miR-200b inhibits proliferation and metastasis of breast cancer by targeting fucosyltransferase IV and alpha1,3-fucosylated glycans. Oncogenesis 2017; 6: e358.

[14] Macedo T, Silva-Oliveira RJ, Silva VAO, Vidal DO, Evangelista AF and Marques MMC. Overexpression of mir-183 and mir-494 promotes proliferation and migration in human breast cancer cell lines. Oncol Lett 2017; 14: 1054-1060.

[15] Zhou B, Shan H, Su Y, Xia K, Zou R and Shao Q. Let-7a inhibits migration, invasion and tumor growth by targeting AKT2 in papillary thyroid carcinoma. Oncotarget 2017; 8: 69746-69755.

[16] Valastyan S. Retraction note to: roles of microRNAs and other non-coding RNAs in breast cancer metastasis. J Mammary Gland Biol Neoplasia 2016; 21: 151.

[17] Liu Y, Wang F and Xu P. miR-590 accelerates lung adenocarcinoma migration and invasion through directly suppressing functional target OLFM4. Biomed Pharmacother 2017; 86: 466-474.

[18] Miao MH, Ji XQ, Zhang H, Xu J, Zhu H and Shao XJ. miR-590 promotes cell proliferation and invasion in T-cell acute lymphoblastic leukaemia by inhibiting RB1. Oncotarget 2016; 7: 39527-39534.

[19] Pang H, Zheng Y, Zhao Y, Xiu X and Wang J. miR-590-3p suppresses cancer cell migration, invasion and epithelial-mesenchymal transition in glioblastoma multiforme by targeting ZEB1 and ZEB2. Biochem Biophys Res Commun 2015; 468: 739-745.

[20] Hong L, Zhao X, Shao X and Zhu H. miR-590 regulates WT1 during proliferation of G401 cells. Mol Med Rep 2017; 16: 247-253.

[21] Ou C, Sun Z, Li X, Li X, Ren W, Qin Z, Zhang X, Yuan W, Wang J, Yu W, Zhang S, Peng Q, Yan Q, Xiong W, Li G and Ma J. MiR-590-5p, a density-sensitive microRNA, inhibits tumorigenesis by targeting YAP1 in colorectal cancer. Cancer Lett 2017; 399: 53-63.
[22] Ge X and Gong L. MiR-590-3p suppresses hepatocellular carcinoma growth by targeting TEAD1. Tumour Biol 2017; 39: 1010428317-695947.
[23] Lorusso G and Ruegg C. New insights into the mechanisms of organ-specific breast cancer metastasis. Semin Cancer Biol 2012; 22: 226-233.
[24] Phillips S and Kuperwasser C. SLUG: critical regulator of epithelial cell identity in breast development and cancer. Cell Adh Migr 2014; 8: 578-587.
[25] Kim J, Bae S, An S, Park JK, Kim EM, Hwang SG, Kim WJ and Um HD. Cooperative actions of p21WAF1 and p53 induce Slug protein degradation and suppress cell invasion. EMBO Rep 2014; 15: 1062-1068.
[26] Christopher AF, Kaur RP, Kaur G, Kaur A, Gupta V and Bansal P. MicroRNA therapeutics: discovering novel targets and developing specific therapy. Perspect Clin Res 2016; 7: 68-74.
[27] Bader AG. miR-34-a microRNA replacement therapy is headed to the clinic. Front Genet 2012; 3: 120.

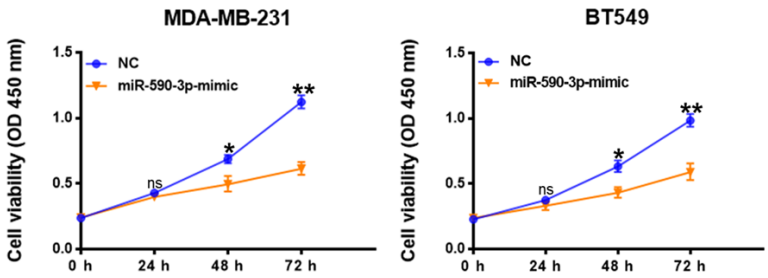

Supplementary Figure 1. Cell proliferation was inhibited by miR-590-3p 48 h after transfection but not 24 h after transfection. CCK8 assay was used to analyze cell proliferation of MDA-MB-231 and BT549 cells with miR-590-3p NC or miR-590-3p mimics transfection. Data represent the mean ± standard error of the mean based on three independent experiments, which were analyzed by two-tailed Student's *t*-test. ns, no significance; *, $P < 0.05$; **, $P < 0.01$.

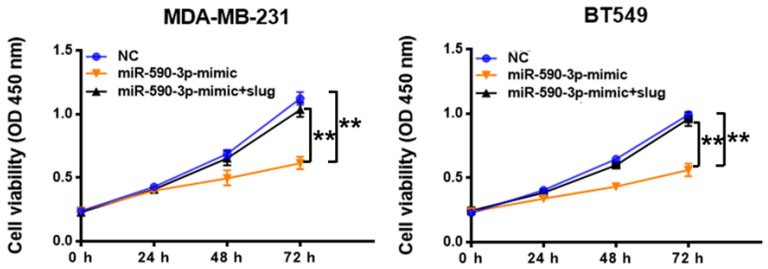

Supplementary Figure 2. Inhibitory effect of miR-590-3p on cell proliferation was completely abolished by Slug. MDA-MB-231 and BT549 cells proliferation after transfection with miR-590-3p-NC or miR-590-3p mimic along with or without the Slug were determined by CCK8 assay. Data represent the mean ± standard error of the mean based on three independent experiments, which were analyzed by two-tailed Student's *t*-test. **, $P < 0.01$.